

In the former case the vibrational levels of the 1A_1 state which are involved are higher energy levels than in the small ΔE_0 case. The probability distributions for higher energy vibrational levels have "tails" which go further into the potential-energy barrier and facilitate tunneling.

Studies are in progress to investigate the effects on the spin-state interconversion rate of added electrolyte, of added analogous Zn^{II} complex, and of changing the solvent to a higher dielectric solvent than acetone. We are also investigating whether part of the change

in apparent Arrhenius activation energy as a function of concentration is not only due to changes in ΔE_0 for a given complex, but may also be due to differences in activation energies to form different-sized aggregates.

Acknowledgment. We are grateful for support from National Institutes of Health Grant HL16352 and discussions with Professor Peter Wolyne and we thank Dr. Bruce S. Brunschwig for pointing out calculational errors in ref 1,

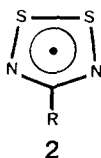
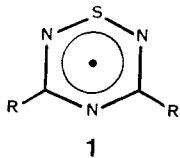
Ultraviolet Photoelectron and ESR Studies of 1,2,4,6-Thiatriazinyl and 1,2,3,5-Dithiadiazolyl Radicals

René T. Boeré, Richard T. Oakley,* Robert W. Reed, and Nicholas P. C. Westwood*

Contribution from the Guelph-Waterloo Centre for Graduate Work in Chemistry, Guelph Campus, Department of Chemistry and Biochemistry, University of Guelph, Guelph, Ontario N1G 2W1, Canada. Received June 24, 1988

Abstract: 1,2,4,6-Thiatriazinyl radicals, $[R_2C_2N_3S]^*$, and 1,2,3,5-dithiadiazolyl radicals, $[RCN_2S_2]^*$ ($R = CF_3, Cl, Ph$), have been generated in the gas phase and studied by He I photoelectron spectroscopy. Thiatriazinyls with $R = CF_3, Cl, 4-MeOC_6H_4,$ and $4-NO_2C_6H_4$ have also been prepared in solution and characterized by ESR spectroscopy. Ionization potential and hyperfine coupling constant data for these radical systems are analyzed in relation to the results of MNDO calculations on their electronic structures; the effects of conjugative interactions between the exocyclic ligand(s) and the heterocyclic ring are more pronounced in the thiatriazinyl system.

Many of the recent developments in heterocyclic thiazene chemistry have been concerned with the generation, energetics of association, and the rearrangements of radical systems.¹ In our work we have focused attention on the properties of 1,2,4,6-thiatriazinyl radicals **1**,²⁻⁴ in particular, the potential use of these



and related derivatives in the design of low-dimensional molecular metals.⁵ To this end we have been concerned with the dependence of molecular properties, e.g., spin distributions and ionization potentials, on the nature of the 3,5-ligands.⁴ Radicals based on the 1,2,3,5-dithiadiazolyl framework **2** have also received considerable attention; derivatives with a variety of R groups have been characterized by ESR spectroscopy,⁶ and the solid-state structures of the radical dimers of **2** ($R = Ph$ and CF_3)^{6a,7} have been reported. The structure of **2** ($R = CF_3$) has also been studied

Table I. Ionization Potentials (eV) of **1**, $[R_2C_2N_3S]^*$, and **2**, $[RCN_2S_2]^*$ ^{a-c}

1, R =			2, R =		
CF ₃	Cl	Ph	CF ₃	Cl	Ph
(8.6)	(8.18)	(6.81)	(7.94)	(7.73)	(7.10)
9.1	8.57	7.35	8.25	8.00	7.40
11.5	11.0 (sh)	8.9 (sh)	11.1	10.27	8.9
12.2	11.29	9.2	11.65	11.0 (sh)	9.4
12.7	12.22	9.4	12.0	11.33	10.2 (sh)
13.7	12.79	10.9	13.23	11.80	10.6
14.6	13.79 (sh)	11.9	14.5	12.30	11.2
15.3 (sh)	14.06	12.8	15.08	12.69	12.1
15.7	15.44	14.1	15.9	13.41	13.0
	17.2	14.6	16.9	15.04	14.1
				16.5	14.9

^aOnsets (assumed adiabatics) for the first IPs in parentheses; all other IPs are vertical, or estimated band maxima in the case of broad/unresolved features. ^bFirst IPs are ± 0.04 eV except for **1** ($R = CF_3$). All other bands are either ± 0.06 or ± 0.1 eV. ^c(sh) refers to a shoulder on the side of a maximum.

in the gas phase by electron diffraction.^{6a}

In order to probe more deeply the electronic structures of **1** and **2**, we have turned to the use of UV photoelectron spectroscopy (UPS). In general, the analysis of radicals by UPS has been restricted. Aside from the usual stable open-shell molecules, e.g., O_2 , NO , NO_2 , most photoelectron studies have focused on extremely short-lived di-, tri-, and tetraatomic radicals,⁸ including NS ,⁹ together with a few assorted organic species, i.e., alkyls,^{8,10} nitroxides,¹¹ benzyl,¹² phenyl,¹³ troyl,¹⁴ and phenoxy.¹⁵ In most

- (1) Oakley, R. T. *Prog. Inorg. Chem.* **1988**, *36*, 299.
- (2) Hayes, P. J.; Oakley, R. T.; Cordes, A. W.; Pennington, W. T. *J. Am. Chem. Soc.* **1985**, *107*, 1346.
- (3) Oakley, R. T.; Reed, R. W.; Cordes, A. W.; Craig, S. L.; Graham, J. B. *J. Am. Chem. Soc.* **1987**, *109*, 7745.
- (4) Boeré, R. T.; Cordes, A. W.; Hayes, P. J.; Oakley, R. T.; Reed, R. W.; Pennington, W. T. *Inorg. Chem.* **1986**, *25*, 2445.
- (5) Haddon, R. C. *Aust. J. Chem.* **1975**, *28*, 2343.
- (6) (a) Höfs, H.-U.; Bats, J. W.; Gleiter, R.; Hartmann, G.; Mews, R.; Eckert-Maksić, M.; Oberhammer, H.; Sheldrick, G. M. *Chem. Ber.* **1985**, *118*, 3781. (b) Markovskii, L. N.; Polumbrik, P. M.; Talanov, V. S.; Shermolovich, Yu. G. *Tetrahedron Lett.* **1982**, *23*, 761. (c) Müller, T. Dissertation, University of Frankfurt, 1979. (d) Fairhurst, S. A.; Johnson, K. M.; Sutcliffe, L. H.; Preston, K. F.; Banister, A. J.; Hauptmann, Z. V.; Passmore, J. *J. Chem. Soc., Dalton Trans.* **1986**, 1465.
- (7) Vegas, A.; Pérez-Salazar, A.; Banister, A. J.; Hey, R. G. *J. Chem. Soc., Dalton Trans.* **1980**, 1812.

- (8) Dyke, J. M.; Jonathan, N.; Morris, A. *Int. Rev. Phys. Chem.* **1982**, *2*, 3.
- (9) Dyke, J. M.; Morris, A.; Trickle, I. R. *J. Chem. Soc., Faraday Trans. 2* **1977**, *73*, 147.
- (10) Dearden, D. V.; Beauchamp, J. L. *J. Phys. Chem.* **1985**, *89*, 5359, and references therein.
- (11) Morishima, I.; Yoshikawa, K.; Yonezawa, T.; Matsumoto, H.; *Chem. Phys. Lett.* **1972**, *16*, 336.

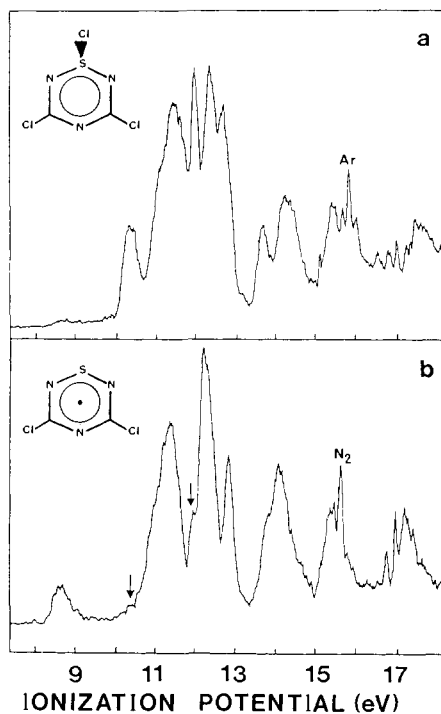


Figure 1. He I photoelectron spectra of (a) 1-chloro-1,2,4,6-thiatriazine, $\text{Cl}_2\text{C}_2\text{N}_3\text{SCl}$, and (b) the radical product **1** ($\text{R} = \text{Cl}$) produced by passage of $\text{Cl}_2\text{C}_2\text{N}_3\text{SCl}$ over Ag wool at 1 Torr and 200 °C. Arrows in (b) indicate traces of the starting material.

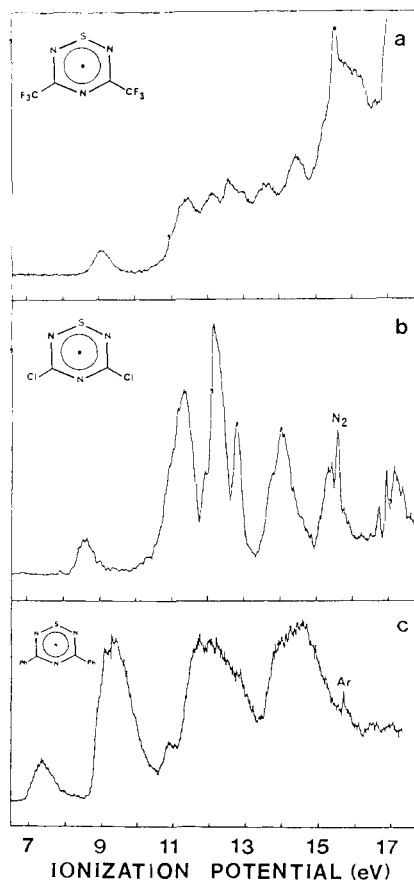


Figure 2. He I photoelectron spectra of the 1,2,4,6-thiatriazinyl radicals $[\text{R}_2\text{C}_2\text{N}_3\text{S}]^*$ (**1**) with $\text{R} = \text{CF}_3$ (a), Cl (b), and Ph (c). Experimental conditions: (a) on-line reduction of the 1-chloro derivative over Ph_3Sb at room temperature, (b) as summarized in Figure 1, (c) from the vapor above the radical dimer at 95 °C in a heated probe.

cases only the first ionization potentials (IPs) are observed, the remainder of the spectrum being obscured by precursor molecules

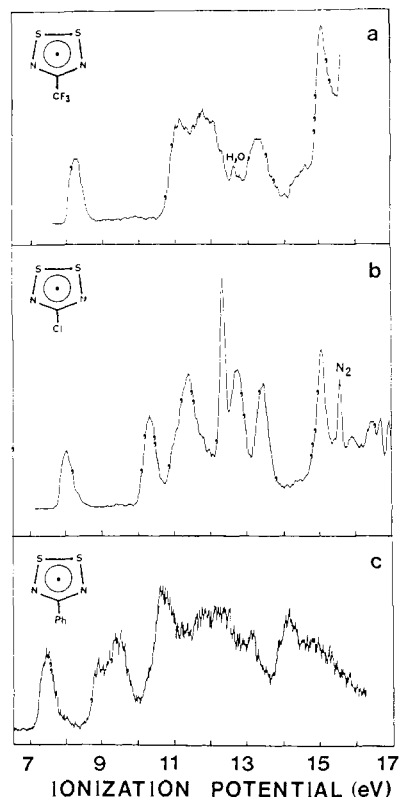


Figure 3. He I photoelectron spectra of the 1,2,3,5-dithiadiazolyl radicals $[\text{RCN}_2\text{S}_2]^*$ (**2**) with $\text{R} = \text{CF}_3$ (a), Cl (b), and Ph (c). Experimental conditions: (a) and (b) from the vapor above the radical dimer at room temperature, (c) from the vapor above the radical dimer at 65 °C in a heated probe.

and/or stable products. Studies on large inorganic radicals are particularly rare, the recently observed $[\text{S}_3\text{N}_3]^*$ being a notable exception.¹⁶ The present study on **1** and **2** thus provides a unique opportunity to investigate and compare complementary gas-phase photoelectron and solution ESR spectroscopic data on two series of heterocyclic radicals.

Results

Generation and Photoelectron Spectra of 1 and 2. In seeking ionization potential data on thiatriazinyls **1** and dithiadiazolyls **2** we have been limited to examples which can be readily vaporized into a photoelectron spectrometer. Moreover, in order to make a more meaningful comparison between the two radical systems **1** and **2**, we have restricted our study to derivatives with the same R groups, i.e., $\text{R} = \text{CF}_3$, Cl , and Ph . We have utilized two spectrometers: (i) a home-built fast pumping model¹⁷ suitable for relatively volatile samples ($\text{R} = \text{CF}_3$, Cl), and (ii) a modified Perkin-Elmer PS 16/18 instrument with a heated probe for less volatile samples ($\text{R} = \text{Ph}$). In the case of the thiatriazinyls **1**, samples were admitted in two ways: (i) on-line reduction of the corresponding 1-chlorothiatriazines over heated silver wool (for $\text{R} = \text{Ph}$ or Cl), or at ambient temperature over triphenylantimony (for $\text{R} = \text{CF}_3$ or Cl); and (ii) direct sampling of the vapor over the radical dimer ($\text{R} = \text{Ph}$). This latter technique was used exclusively for the dithiadiazolyls **2**. An example of the changes occurring during reduction of $\text{Cl}_2\text{C}_2\text{N}_3\text{SCl}$ over Ag wool is shown in Figure 1.

(12) Hayashibara, K.; Kruppa, G. H.; Beauchamp, J. L. *J. Am. Chem. Soc.* **1986**, *108*, 5441.

(13) Butcher, V.; Costa, M. L.; Dyke, J. M.; Ellis, A. R.; Morris, A. *Chem. Phys.* **1987**, *115*, 261.

(14) Koenig, T.; Chang, J. C. *J. Am. Chem. Soc.* **1978**, *100*, 2240.

(15) Dewar, M. J. S.; David, D. E. *J. Am. Chem. Soc.* **1980**, *102*, 7387.

(16) Lau, W. M.; Westwood, N. P. C.; Palmer, M. H. *J. Am. Chem. Soc.* **1986**, *108*, 3229.

(17) Sammynaiken, R. M.Sc. Thesis, University of Guelph, 1988.

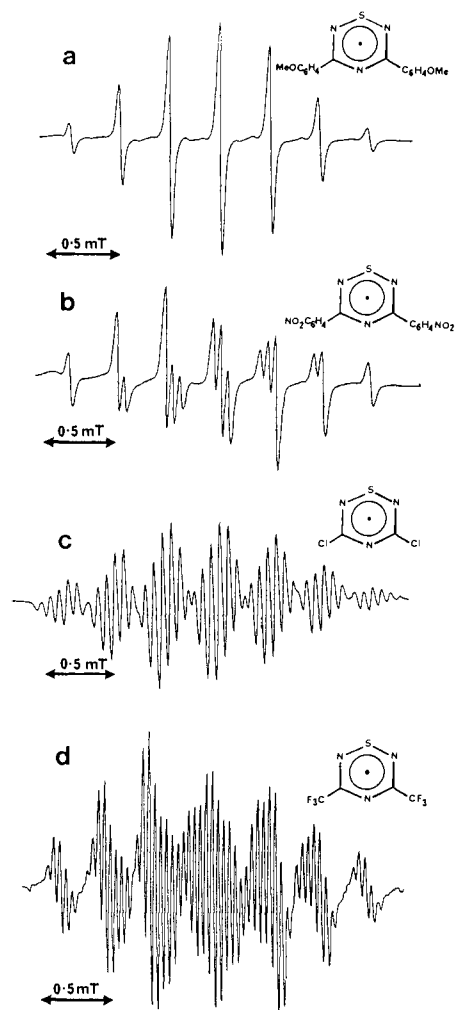


Figure 4. ESR spectra (in CH_2Cl_2) of 1,2,4,6-thiatriazinyl radicals $[\text{R}_2\text{C}_2\text{N}_3\text{S}]^*$ (**1**) with $\text{R} = 4\text{-MeOC}_6\text{H}_4$ (a), $4\text{-NO}_2\text{C}_6\text{H}_4$ (b), Cl (c), and CF_3 (d).

The photoelectron spectra collected in Figures 2 and 3 are essentially those of pure radicals, indicating the efficacy of the sampling procedures. Traces of N_2 , Ar, and H_2O are labeled in some spectra. Note that for **1** and **2** ($\text{R} = \text{Ph}$) a decrease in intensity at low kinetic energy is observed; this is a function of the different sweep methods for the PS 16/18 and the home-built instrument. Instrumental resolution was maintained at 45 meV during the course of these experiments. For each system the spectrum is characterized by a single weak, low-energy ionization band followed, after a gap, by many higher IPs. Vertical IPs up to 16–17 eV are compiled in Table I. In the $\text{R} = \text{CF}_3$ and Ph species, only estimated band maxima are quoted owing to a high density of states.

To facilitate tentative assignments, and to provide an assessment of the electronic structures of **1** and **2**, MNDO calculations were performed on the radicals and the corresponding ground-state cations. The results of this analysis are provided below.

ESR Spectra of 1. 1,2,4,6-Thiatriazinyl radicals were first reported by Kornuta and co-workers, using ESR spectroscopy.¹⁸ Their procedure for generating the radicals involved the reduction of the corresponding 1-chlorothiatriazines by either sodium verdaeryl or zinc powder. In our study of the preparation and association of the 3,5-diphenyl radical **1** ($\text{R} = \text{Ph}$) and the analogous selenium compound, we have used the same approach but have found triphenylantimony to be a faster and more convenient reagent.²³ In the present study we have continued with this latter reagent and have extended the family of known radicals to include

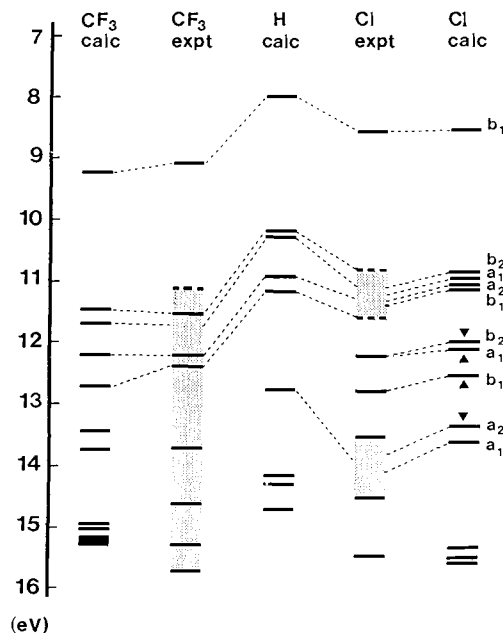


Figure 5. Correlation diagram for $[\text{R}_2\text{C}_2\text{N}_3\text{S}]^*$ radicals **1**. A comparison of the calculated orbital energies (MNDO RHF values uniformly reduced by 1.5 eV) and experimental IPs for $\text{R} = \text{CF}_3$ and Cl. Exchange splittings are assumed to be small. Calculations for the H-substituted species are also shown. Hatched areas correspond to broad bands or continua containing multiple IPs. Those orbitals with a preponderance of halogen character are indicated by an arrowhead; the remainder are essentially ring-based orbitals.

Table II. ESR Hyperfine Coupling Constants (in mT) for **1**, $[\text{R}_2\text{C}_2\text{N}_3\text{S}]^*$

R	<i>g</i>	<i>a</i> (N2, 6)	<i>a</i> (N4)
Ph ^a	2.0059	0.397	0.397
4-MeOC ₆ H ₄	2.0064	0.365	0.365
4-NO ₂ C ₆ H ₄	2.0055	0.372	0.427
Cl ^b	2.0055	0.345	0.415
CF ₃ ^c	2.0065	0.335	0.459

^a Reference 3. ^b *a*(Cl) = 0.062 mT. ^c *a*(F) = 0.042 mT.

$\text{R} = 4\text{-MeOC}_6\text{H}_4$, $4\text{-NO}_2\text{C}_6\text{H}_4$, Cl, and CF_3 . Figure 4 shows the ESR spectra of the thiatriazinyls of these species, as recorded at room temperature in methylene chloride. The isotropic hyperfine coupling data presented in Table II were determined by spectral simulation methods.¹⁹

Discussion

The electronic structures of both 1,2,4,6-thiatriazinyls and 1,2,3,5-dithiadiazolyls have been studied by several groups.^{2–4,6} MNDO analyses of the model systems $[\text{H}_2\text{C}_2\text{N}_3\text{S}]^*$ (**1**, $\text{R} = \text{H}$) and $[\text{HCN}_2\text{S}_2]^*$ (**2**, $\text{R} = \text{H}$) have confirmed that both are 7π -electron radicals, with ${}^2\text{B}_1$ and ${}^2\text{A}_2$ ground states, respectively. In Figures 5 and 6 we compare the MNDO/HE eigenvalues for the radicals $[\text{R}_2\text{C}_2\text{N}_3\text{S}]^*$ (**1**) and $[\text{RCN}_2\text{S}_2]^*$ (**2**, $\text{R} = \text{H}, \text{Cl}, \text{CF}_3$) with the IPs observed in **1** and **2** ($\text{R} = \text{CF}_3, \text{Cl}$). The model calculations are not intended to provide an absolute correspondence, via Koopmans' theorem,²⁰ between the orbital energies and the observed ionization potentials. They do, however, provide a framework within which to compare the common and distinct features of the two radical systems. Indeed, although the doublet correction in the HE method gives first IPs that are some 1.5–2.0 eV too high, the calculated orbital energies (when collectively reduced by 1.5 eV) show a remarkably close correspondence to the experimental spectra, such that groups of orbitals can be tentatively identified.

(18) Markovskii, L. N.; Kornuta, P. P.; Katchkovskaya, L. S.; Polumbrik, P. M. *Sulfur Lett.* **1983**, *1*, 143.

(19) ESR spectral simulations were performed with ESR42, a program written by U. Oehler, University of Guelph. See: Oehler, U. M.; Janzen, E. G. *Can. J. Chem.* **1982**, *60*, 1542.

(20) Richards, W. G. *Int. J. Mass Spectrom. Ion Phys.* **1969**, *2*, 419.

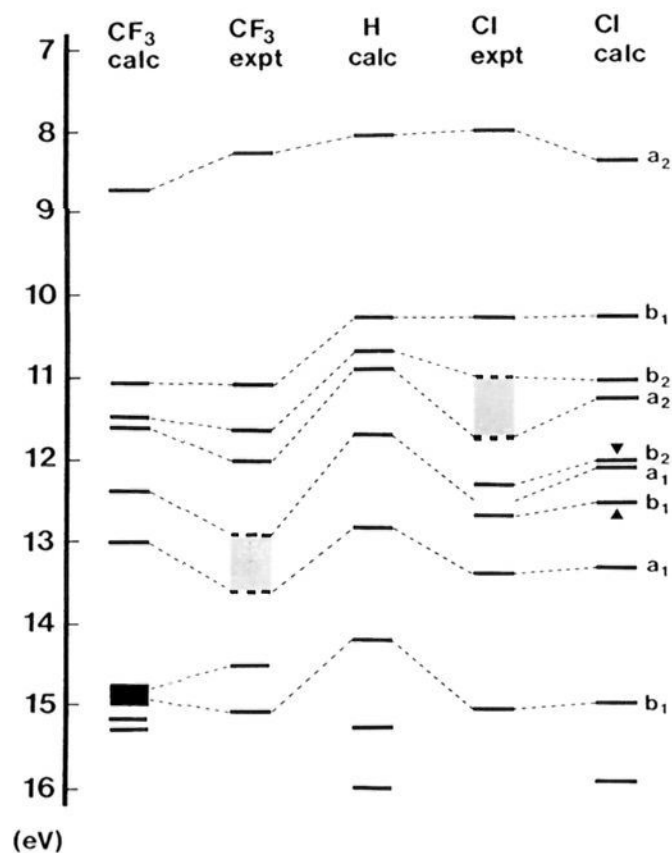
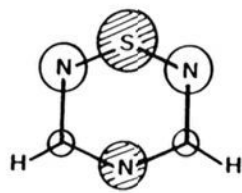


Figure 6. Correlation diagram for $[\text{RCN}_2\text{S}_2]^*$ radicals **2**. A comparison of the calculated orbital energies (MNDO RHF values uniformly reduced by 1.5 eV) and experimental IPs for $\text{R} = \text{CF}_3$ and Cl . Exchange splittings are assumed to be small. Calculations for the H-substituted species are also shown. Hatched areas correspond to broad bands or continua containing multiple IPs. Those orbitals with a preponderance of halogen character are indicated by an arrowhead; the remainder are essentially ring-based orbitals.

Chart I



The photoelectron spectra of both **1** and **2** can be broken into three distinct regions, corresponding to ionization of electrons from (i) the low-lying SOMO (7–9 eV), (ii) the π - and σ -orbitals associated with the heterocyclic ring, and (iii) the orbitals associated with the ligands CF_3 , Cl , and Ph . The first two regions can be correlated with the MNDO results for the unsubstituted species ($\text{R} = \text{H}$). The characteristics of the first IP between the two series is particularly noteworthy. For a given R group the thiatriazinyl IPs are slightly higher than those of the dithiadiazolyls, suggesting a more electronegative core for the former. In addition, the adiabatic/vertical difference is smaller for the thiatriazinyls (0.3 eV) than for the dithiadiazolyls (0.5 eV), indicating a smaller geometry change upon ionization.²¹ The most important point, however, is that the spread in the first IPs for the thiatriazinyls (1.75 eV) is significantly larger than in the dithiadiazolyls (0.84 eV). This difference can be rationalized at the one-electron level in terms of the symmetry properties of the SOMOs of the model radicals (Chart I). The vertical nodal plane in the a_2 SOMO of $[\text{HCN}_2\text{S}_2]^*$ bisects the molecule and prohibits direct conjugative interaction between the ligand and the unpaired electron.

This conclusion is supported by comparison of the spin distributions in **1** and **2**, as reflected by the magnitudes of the hy-

(21) The atomic constitutions of thiatriazinyls and dithiadiazolyls are clearly different. It is nonetheless instructive to compare the properties of these systems in terms of two homoatomic 7π rings composed of six and five atoms, respectively. For example, the Hückel SOMO energy of a six-membered 7π ring is given by $\alpha + 2\beta \cos(4\pi/6)$, while that of a five-membered 7π ring is $\alpha + 2\beta \cos(4\pi/5)$ (where α and β have their usual meaning); accordingly **2** should be more electron-rich, that is, more easily ionized, than **1**. Similarly the antibonding properties of the SOMO in **2** should be more severe than in **1** (two nodal planes spread over five linkages as opposed to six).

Table III. ESR Coupling Constants (in mT) for **2**, $[\text{RCN}_2\text{S}_2]^*$

R	$a(\text{N})$	ref	R	$a(\text{N})$	ref
F	0.506	6a	CF_3	0.51	6a
Cl	0.53	6a	CCl_3	0.49	6b
Br	0.5	6a	<i>t</i> -Bu	0.5	6c
Ph	0.49	6b	Me	0.49	6d

Table IV. Calculated (MNDO) and Experimental First IPs (eV) for the Radical Series $[\text{R}_2\text{C}_2\text{N}_3\text{S}]^*$ (**1**) and $[\text{RCN}_2\text{S}_2]^*$ (**2**), $\text{R} = \text{CF}_3$ and Ph

	calcd IPs			exptl IPs
	HE ^a	ΔSCF^b	EA, cation ^b	
1 , $\text{R} = \text{CF}_3$	10.73	10.75	10.50	9.1
1 , $\text{R} = \text{Cl}$	10.07	9.73	9.58	8.57
2 , $\text{R} = \text{CF}_3$	10.17	9.98	9.96	8.25
2 , $\text{R} = \text{Cl}$	9.85	9.62	9.52	8.00

^aOrbital energies with correction for mutual self-repulsion of two half electrons. ^bVertical IPs.

perfine coupling constants to the endocyclic nitrogens, a_{N} . Accordingly, spin density in the thiatriazinyl systems is equally distributed over the three nitrogens when $\text{R} = \text{Ph}$ or $4\text{-MeOC}_6\text{H}_4$, but becomes strongly polarized toward the N_4 position when electron-withdrawing groups ($\text{R} = \text{Cl}$, $4\text{-NO}_2\text{C}_6\text{H}_4$, CF_3) are present (Table II).²² By contrast, dithiadiazolyl radicals exhibit hyperfine coupling constants which are practically invariant to the nature of R (Table III).

Beyond the first IP, the PE spectra are complicated by the doubling of bands (triplet and singlet) for each successive cationic state; indeed in many of the spectra weak shoulders are observed which could be assigned to singlet states associated with a lower energy triplet. Given the richness of the spectra it would be premature at this point to attempt to establish the exchange splittings for these states. From the extent of delocalization it seems reasonable to assume that these are small, as illustrated in Figure 1, where the new spectrum (b), apart from the distinct SOMO, is not markedly different from that of the precursor (a). These spectra also indicate that the ring orbitals are only marginally perturbed upon radical formation. Figures 5 and 6 show a reasonable correlation for the higher IPs of the radicals, based on the establishment of the locations for the ligand-based orbitals. Clearly the cluster of bands around 9.2 eV in both **1** and **2** ($\text{R} = \text{Ph}$) originate from the phenyl groups (Figures 2 and 3). Likewise the bands observed in the 12–13.5-eV region in the chloro derivatives can be assigned to ligand ionizations; indeed, the distinct sharp peak at 12.3 eV in **2** ($\text{R} = \text{Cl}$) and the somewhat broader band in **1** ($\text{R} = \text{Cl}$) at 12.2 eV are classic examples of ionization from chlorine 3p "lone-pair" orbitals.

The remaining bands in **2** at 11–12 eV ($\text{R} = \text{CF}_3$), 10.3 and 11.3 eV ($\text{R} = \text{Cl}$), and 10.6 (and possibly 11.2) eV ($\text{R} = \text{Ph}$) are then associated with the π (b_1 , a_2) and σ (b_2) orbitals of the ring. The unique band with the somewhat lower IP (10.3 eV) observed for $\text{R} = \text{Cl}$ can be assigned to a b_1 orbital which is destabilized through interaction with a Cl p_π lone pair. These ring orbitals are also discernible in the **1** series, at 11.5 eV and up ($\text{R} = \text{CF}_3$), around 11.3 eV ($\text{R} = \text{Cl}$) and at 11.9 eV ($\text{R} = \text{Ph}$), although they are predictably more complex. Higher IPs for the CF_3 and Ph species are unassignable; however, in **2** ($\text{R} = \text{CF}_3$ and Cl) the unique bands near 13.3 and 15.0 eV can be tentatively attributed to the σ -bonding a_1 and lowest π -bonding orbital $1b_1$. The MNDO calculations indicate that these orbitals are relatively ligand invariant. In **1** ($\text{R} = \text{Cl}$) the broad band centered at 14.1 eV probably involves a contribution from a Cl based orbital (a_2) and an a_1 ring orbital (Figure 5).

As mentioned earlier, the first IPs are not well determined by the MNDO/HE method. We have therefore estimated values

(22) We have not included in Table II the preliminary coupling constants reported by Kornuta and co-workers (ref 18). Attempts to correlate these data with our own have led us to conclude that the tentative assignments provided by these workers may be in error.

for these IPs by the Δ SCF technique, i.e., $\Delta H_f(\text{cation}) - \Delta H_f(\text{radical})$ with similar (RHF) wave functions, and with all cation calculations carried out at the frozen radical geometry. These give better values for the vertical IPs, as do those established from the electron affinity (EA) of the cation.²³ Table IV shows the results which indicate that all the calculated values are still high, although the experimental differences between the CF_3 and Cl IPs are best reproduced by the HE method.

As a final point it should be noted that the ultraviolet photoelectron spectra of **1** and **2** correspond to the manifold of excited states of the corresponding cations. It is therefore feasible to make a comparison between UV spectroscopic data on the cations (where known) and the energy differences between the first adiabatic IP (ground ionic state) and the higher vertical IPs (excited singlet states) of the radical. Although we are unable to establish exact positions for the excited singlet cations in **1**, we can make reasonable estimates for the **2** series, arriving at ring $\pi-\pi^*$ transitions of 3.16 eV (392 nm), 3.27 eV (379 nm), and 3.2 eV (387 nm) for the CF_3 , Cl, and Ph compounds, respectively. These numbers compare favorably with the known λ_{max} of 396 (CH_2Cl_2)²⁴ or 370 nm (CH_3CN)²⁵ on the $\text{PhCN}_2\text{S}_2^+$ species.

Summary and Conclusion

We have demonstrated herein that radicals of the types **1** and **2** can be generated essentially pure in the gas phase. The IP trends in the photoelectron spectra are tracked surprisingly well by MNDO/HE calculations despite the nonvalidity of Koopmans' theorem. This has permitted tentative, but reasonable, assignments for some of the higher IPs. Taken together the photoelectron and ESR data emphasize that the effects of conjugative interactions between ligand and ring in heterocyclic radicals based on 1,2,4,6-thiatriazinyl and 1,2,3,5-dithiadiazolyl frameworks are notably different. Gas-phase IPs and ESR hyperfine coupling constant data on a series of radicals from each class indicate that the properties of dithiadiazolyls are far less responsive to "fine-tuning" by the ligand environment. In the context of designing neutral radicals as templates for molecular metals, the thiatriazinyl system appears to be a potentially more flexible unit.

Experimental Section

Reagents and General Procedures. The nitriles RCN with $\text{R} = 4\text{-MeOC}_6\text{H}_4$, $4\text{-NO}_2\text{C}_6\text{H}_4$ (Aldrich), and $\text{R} = \text{CF}_3$ (PCR), trifluoroacetamide (Fairfield), benzamidine hydrochloride (Aldrich), sulfur monochloride and dichloride (Aldrich), thionyl chloride (Aldrich), and sodium dicyanoamide (Aldrich) were obtained commercially. All, save the sulfur and thionyl chlorides, which were freshly distilled before use, were used as received. The amidines $\text{RC}(\text{NH})\text{NH}_2$ ($\text{R} = 4\text{-MeOC}_6\text{H}_4$, $4\text{-NO}_2\text{C}_6\text{H}_4$), the chlorothiatriazines **3** ($\text{R} = \text{Cl}$ and Ph),^{2,26} and $\text{S}_3\text{N}_3\text{Cl}_3$ ²⁷ were all prepared according to literature methods.

Unless otherwise specified all synthetic procedures were carried out under a nitrogen atmosphere. All solvents were of reagent grade; acetonitrile and methylene chloride were dried by distillation from P_2O_5 prior to use. Chemical analyses were performed by MHW Laboratories, Phoenix, AZ. Melting points (uncorr) were determined on a Gallenkamp melting point apparatus. Infrared spectra were recorded (with CsI cells) on a Nicolet 20SXC FTIR spectrometer. Low-resolution EI (70 eV) mass spectra were obtained on a VG 7070 EF spectrometer, samples being admitted through conventional inlet systems. ESR spectra were recorded using a Varian E104 spectrometer.

Preparation of 1-Chloro-1,2,4,6-thiatriazines 3. (i) $\text{R} = 4\text{-MeOC}_6\text{H}_4$. 4-Methoxybenzamidine (2.48 g, 16.5 mmol) was combined with $\text{S}_3\text{N}_3\text{Cl}_3$ (1.62 g, 6.62 mmol) in 50 mL of acetonitrile and the mixture heated at gentle reflux for 16 h. The mixture was then hot-filtered and the filtrate cooled to 0 °C. The crystalline precipitate was filtered off and heated

at 70 °C (0.01 Torr) to sublime out traces of S_4N_4 . The remaining solid was then extracted with hot carbon tetrachloride, the extracts filtered, and the filtrate reduced to dryness in vacuo. The residue was recrystallized from acetonitrile to yield orange moisture-sensitive needles of **3** ($\text{R} = 4\text{-MeOC}_6\text{H}_4$), 0.55 g (1.58 mmol): mp 160 °C; IR (Nujol mull, 2000–250 cm^{-1}) 1600 (s), 1575 (w), 1458 (m), 1441 (m), 1380 (s), 1318 (s), 1300 (w), 1260 (s), 1183 (w), 1164 (s), 1118 (m), 1106 (w), 1026 (m), 970 (m), 848 (m), 784 (m), 571 (m), 540 (m), 450 (m), 400 (m), 330 (w), 310 (m) cm^{-1} ; mass spectrum m/e 312 ($(4\text{-MeOC}_6\text{H}_4)_2\text{C}_2\text{N}_3\text{S}^+$, 8%), 179 ($4\text{-MeOC}_6\text{H}_4\text{CN}_2\text{S}^+$, 13%), 133 ($4\text{-MeOC}_6\text{H}_4\text{CN}^+$, 100%). Anal. Calcd for $\text{C}_{16}\text{H}_{14}\text{N}_3\text{O}_2\text{SCl}$: C, 55.25, H, 4.06; N, 12.08; Cl, 10.19. Found: C, 55.31; H, 4.26; N, 12.21; Cl, 9.99.

(ii) $\text{R} = 4\text{-NO}_2\text{C}_6\text{H}_4$. 4-Nitrobenzamidine (5.00 g, 30.3 mmol) was combined with $\text{S}_3\text{N}_3\text{Cl}_3$ (2.50 g, 10.2 mmol) in 75 mL of acetonitrile; the mixture was heated to reflux for 2 h. The mixture was then hot-filtered and the filtrate cooled to 0 °C. The crystalline precipitate was filtered off and heated at 70 °C (0.01 Torr) to sublime out traces of S_4N_4 . The remaining solid was then extracted with hot carbon tetrachloride, the extracts filtered, and the filtrate reduced to dryness in vacuo. The residue was recrystallized as yellow, moisture-sensitive needles of **3** ($\text{R} = 4\text{-NO}_2\text{C}_6\text{H}_4$), 1.00 g (2.6 mmol); dec >170 °C; IR (Nujol mull, 2000–250 cm^{-1}) 1517 (s), 1420 (s), 1405 (m), 1347 (s), 1329 (s), 1172 (w), 1108 (m), 1010 (m), 975 (w), 878 (w), 868 (m), 791 (m), 734 (s), 714 (s), 698 (w), 565 (m), 541 (m), 539 (m), 508 (w), 495 (w), 437 (w), 407 (m), 383 (w), 301 (m), 264 (m) cm^{-1} ; mass spectrum m/e 342 ($(4\text{-NO}_2\text{C}_6\text{H}_4)_2\text{C}_2\text{N}_3\text{S}^+$, 17%), 311 ($(4\text{-NO}_2\text{C}_6\text{H}_4)_2\text{C}_2\text{N}_3\text{H}^+$, 6%), 149 ($4\text{-NO}_2\text{C}_6\text{H}_4\text{CN}^+$, 5%), 46 (NS^+ , 100%). Anal. Calcd for $\text{C}_{14}\text{H}_8\text{N}_4\text{O}_4\text{SCl}$: Cl, 9.4. Found: Cl, 9.3.²⁸

(iii) $\text{R} = \text{CF}_3$. *N*-(Perfluoroacetimidoyl)perfluoroacetamide was prepared in quantitative yield from perfluoroacetonitrile and ammonia by following the procedure of Brown and Schuman.²⁹ The white low-melting solid was not isolated but was retained in the reactor (a Carius tube fitted with a 10-mm Rotaflo valve), into which was distilled 10 mL of CFCl_3 . The mixture was allowed to warm to room temperature in order to allow the imidoamidine to disperse into the solvent. A fivefold excess of sulfur dichloride was then distilled into the reactor, which was then sealed and warmed to 0 °C for 1 h, after which time the orange reaction mixture was fractionated through a -24 °C trap into a -78 °C trap under dynamic vacuum. A second identical fractionation of the contents of the -24 °C trap afforded crude **3** ($\text{R} = \text{CF}_3$) which was further purified by atmospheric fractional distillation to give a pale yellow liquid, bp 129 °C, yield 25% based on ammonia: IR (2000–250 cm^{-1}) 1540 (s), 1450 (m), 1390 (s), 1320 (s), 1230–1170 (s, b), 1130 (m), 990 (w), 850 (m), 810 (s), 800 (w), 740 (w), 690 (s) cm^{-1} . Anal. Calcd for $\text{C}_4\text{ClF}_6\text{N}_3\text{S}$: Cl, 13.1. Found: Cl, 13.1.

Preparation of Dithiadiazolyls 2 ($\text{R} = \text{CF}_3$, Cl, Ph). The dithiadiazolium chloride salts **4** were prepared by the reaction of (i) trifluoroacetamide with SCl_2 (for $\text{R} = \text{CF}_3$), (ii) bis(trimethylsilyl)carbodiimide with SCl_2 ³⁰ (for $\text{R} = \text{Cl}$), and (iii) benzamidine and SCl_2 (for $\text{R} = \text{Ph}$).³¹ The salts were identified by comparison of their principal infrared spectral bands with those reported in the literature.^{6a,26} Generation of the radicals **2** ($\text{R} = \text{CF}_3$, Cl) was carried out according to literature methods^{6a,7} or, in the case of $\text{R} = \text{Ph}$, by the reduction of $\text{PhCN}_2\text{S}_2^+ \text{Cl}^-$ with triphenylantimony. The radical dimers were isolated prior to admission into the photoelectron spectrometer.

Generation of Thiatriazinyls 1 in Solution. The thiatriazinyl radicals **1** were generated in solution by addition of excess of triphenylantimony to a dilute ($<10^{-4}$ M) solution of the corresponding 1-chlorothiatriazine **3** in methylene chloride. Solutions of **1** were thoroughly purged of oxygen in a stream of argon prior to ESR analysis.

MNDO Calculations. The reported MNDO half-electron (HE) eigenvalues for the **1** and **2** radicals ($\text{R} = \text{H}$, Cl, and CF_3) stem from restricted Hartree-Fock (RHF) calculations in which full geometry optimization within C_{2v} symmetry (C , for $\text{R} = \text{CF}_3$) was invoked. The cation energies were calculated at the corresponding radical geometries. The calculations were performed using the MOPAC suite of programs,³² running on a SUN-3 workstation.

Acknowledgment. We thank the Natural Sciences and Engineering Research Council for support in the form of operating

(23) Dewar, M. J. S.; Kollmar, H. W.; Suck, S. H. *Theor. Chim. Acta* 1975, 36, 237.

(24) Alange, G. G.; Banister, A. J.; Bell, B.; Millen, P. W. *J. Chem. Soc., Perkin Trans. 1* 1979, 1192.

(25) Chivers, T.; Edelmann, F.; Richardson, J. F.; Smith, N. R. M.; Treu, O.; Trsic, M. *Inorg. Chem.* 1986, 25, 2119.

(26) (a) Geever, J.; Hackmann, J. Th.; Trompen, W. P. *J. Chem. Soc. C* 1970, 875. (b) Schramm, W.; Voss, G.; Rembasz, G.; Fischer, E. *Z. Chem.* 1974, 14, 471. (c) Schramm, W.; Voss, G.; Michalik, M.; Rembasz, G. *Z. Chem.* 1975, 15, 19.

(27) Alange, G. G.; Banister, A. J.; Bell, B. *J. Chem. Soc., Dalton Trans.* 1972, 2399.

(28) Repeated attempts failed to provide a satisfactory C, H, N analysis for this compound. Its composition, as indicated, is based on a good chlorine analysis, mass spectral evidence, and subsequent ESR data on the reduction product.

(29) Brown, H. C.; Schuman, P. D. *J. Org. Chem.* 1963, 28, 1122.

(30) Höfs, H.-U.; Mews, R.; Clegg, W.; Noltemeyer, M.; Schmidt, M.; Sheldrick, *Chem. Ber.* 1983, 116, 416.

(31) Roessky, H. W.; Müller, T. *Chem. Ber.* 1978, 111, 2960.

(32) (a) Dewar, M. J. S.; Thiel, W. *J. Am. Chem. Soc.* 1977, 99, 4899. (b) *QCPE* 1984, No. 455 (MOPAC).

grants to R.T.O. and N.P.C.W. and a postdoctoral fellowship to R.T.B.

Registry No. 1 (R = H), 118436-74-1; 1 (R = CF₃), 118436-72-9; 1 (R = Cl), 118436-69-4; 1 (R = Ph), 118436-79-6; 1 (R = 4-MeOC₆H₄), 118436-80-9; 1 (R = 4-NO₂C₆H₄), 118436-78-5; 2 (R = H), 118436-73-0; 2 (R = CF₃), 118436-71-8; 2 (R = Cl), 118436-67-2; 2 (R = F), 118436-68-3; 2 (R = Br), 118436-66-1; 2 (R = Ph), 118436-77-4; 2 (R = CCl₃), 118436-70-7; 2 (R = Bu-*t*), 118436-76-3; 2 (R = Me),

118436-75-2; 3 (R = Ph), 94426-38-7; 3 (R = 4-MeOC₆H₄), 118377-76-7; 3 (R = NO₂C₆H₄), 118377-77-8; 3 (R = Cl), 58589-34-7; 3 (R = CF₃), 118377-78-9; 4 (R = F), 99344-85-1; 4 (R = Cl), 85175-36-6; 4 (R = Br), 99344-91-9; 4 (R = Ph), 63481-05-0; 4 (R = CF₃), 93842-58-1; 4 (R = CCl₃), 62635-18-1; 4 (R = Bu-*t*), 63432-63-3; 4 (R = Me), 82290-16-2; S₃N₃Cl₃, 5964-00-1; CFC₃, 75-69-4; 4-methoxybenzamidine, 22265-37-8; 4-nitrobenzamidine, 25412-75-3; *N*-(perfluoroacetimidoyl)perfluoroacetamide, 675-05-8; sulfur dichloride, 10545-99-0.

Polymerization and Decomposition of Acetaldehyde on Ru(001)

M. A. Henderson, Y. Zhou, and J. M. White*

Contribution from the Department of Chemistry, University of Texas, Austin, Texas 78712.
Received July 8, 1988

Abstract: The polymerization and decomposition of acetaldehyde (CH₃CHO) on Ru(001) was studied by high-resolution electron energy loss spectroscopy (HREELS), static secondary ion mass spectrometry (SSIMS), and temperature-programmed desorption (TPD). Evidence is presented that low exposures (<0.4 langmuir) of CH₃CHO on Ru(001) at 110 K polymerize across the surface in two dimensions upon adsorption. $\eta^1(\text{O})$ CH₃CHO, which is the proposed intermediate in surface polymerization, is stable only at exposures approaching saturation of the first layer (0.4–0.6 langmuir). This species incorporates into the surface polymer after heating above 150 K. Exposures above 0.6 langmuir result in multilayer CH₃CHO, which desorbs in TPD at 148 K. A second CH₃CHO state appears in TPD at 250 K for CH₃CHO exposures above 2 langmuir and is attributed to decomposition of polymerized CH₃CHO in three dimensions above the surface. Ions from this polymer, containing at least monomer units, are detected in +SSIMS. The surface polymer decomposes to $\eta^2(\text{C,O})$ CH₃CHO after heating above 250 K. Decomposition of the latter species at 315 K evolves H₂ in TPD and leaves CO and small amounts of C_xH and $\eta^2(\text{C,O})$ CH₃CO on the surface.

1. Introduction

Chemisorbed aldehydes have been proposed as key intermediates in the decomposition of primary alcohols on metal surfaces^{1,2} and in secondary reactions of Fischer-Tropsch synthesis leading to oxygenates.¹ The structure of these intermediates is typically an $\eta^2(\text{C,O})$ bound species. McCabe et al.³ proposed this structure as a minority species from acetaldehyde (CH₃CHO) on Pt(S)-[6(11)×(100)], and Anton et al. have observed it for formaldehyde (H₂CO) Ru(001).⁴ Recently, we have observed $\eta^2(\text{C,O})$ CH₃CHO from the hydrogenation of ketene (CH₂CO) on Ru(001).⁵⁻⁷

In a continuing effort to understand the chemistry of small oxygen-containing molecules on metal surfaces, we have studied the interaction of acetaldehyde with Ru(001) by high-resolution electron energy loss spectroscopy (HREELS), positive static secondary ion mass spectrometry (+SSIMS), and temperature-programmed desorption (TPD). We find that CH₃CHO adsorption on Ru(001) at 110 K is very complex, exhibiting at least four different states, attributed to $\eta^1(\text{O})$, two polymerized forms, and multilayer. Decomposition of one of the polymer species at 250 K results in $\eta^2(\text{C,O})$ CH₃CHO. This species is not observed

upon adsorption at 110 K, but it is responsible for all the H₂, CO, and trace CO₂ observed in TPD. Polymerization of CH₃CHO has been observed in hydrocarbon solutions,⁸⁻¹⁴ on oxides,¹⁵ and in matrix media¹⁶ but not without the influence of an inorganic acid or organometallic initiator. In UHV experiments, Madix et al.¹⁷ were the first to observe CH₃CHO polymerization, as the cyclic trimer paraldehyde, from CH₃CHO adsorbed on a p(2×2) S-covered Ni(100) surface.

2. Experimental Section

The ultrahigh-vacuum chamber used in this study and the methods of data collection have been detailed elsewhere.¹⁸ The system is ion-pumped with a working base pressure of 1×10^{-10} Torr. The HREELS

(1) Benziger, J. B.; Madix, R. J. *J. Catal.* **1982**, *74*, 55.
(2) (a) Davis, J. L.; Barteau, M. A. *Surf. Sci.* **1987**, *187*, 387. (b) Davis, J. L.; Barteau, M. A. *Surf. Sci.* **1988**, *197*, 123.
(3) McCabe, R. W.; Dimaggio, C. L.; Madix, R. J. *J. Phys. Chem.* **1985**, *89*, 854.
(4) (a) Anton, A. B.; Parmeter, J. E.; Weinberg, W. H. *J. Am. Chem. Soc.* **1985**, *107*, 5558. (b) Anton, A. B.; Parmeter, J. E.; Weinberg, W. H. *J. Am. Chem. Soc.* **1986**, *108*, 1823.
(5) Henderson, M. A.; Radloff, P. L.; White, J. M.; Mims, C. A. *J. Phys. Chem.* **1988**, *92*, 4111.
(6) Henderson, M. A.; Radloff, P. L.; Greenlief, C. M.; White, J. M.; Mims, C. C. *J. Phys. Chem.* **1988**, *92*, 4120.
(7) Henderson, M. A.; Radloff, P. L.; Greenlief, C. M.; White, J. M.; Mims, C. A. *J. Vac. Sci. Technol., A* **1988**, *6*, 769.

(8) (a) Tani, H.; Yasuda, H.; Araki, T. *J. Polym. Sci.* **1964**, *2B*, 933. (b) Tani, H.; Aoyagi, T.; Araki, T. *J. Polym. Sci.* **1964**, *2B*, 921. (c) Tani, H.; Oguni, N. *J. Polym. Sci.* **1965**, *3B*, 123. (d) Tani, H.; Araki, T.; Yasuda, H. *J. Polym. Sci.* **1966**, *4B*, 727. (e) Yasuda, H.; Tani, H. *Macromolecules* **1973**, *6*, 17.
(9) Ishida, S.-I. *J. Polym. Sci.* **1962**, *62*, 1.
(10) Jenkins, A. D.; Nyathi, J. Z.; Smith, J. D. *Eur. Polym. J.* **1982**, *18*, 149.
(11) Yamamoto, T.; Konagaya, S.; Yamamoto, A. *J. Polym. Sci., Polym. Lett. Ed.* **1978**, *16*, 7.
(12) Vogl, O. *J. Polym. Sci.* **1964**, *2A*, 4591.
(13) Natta, G.; Mazzanti, G.; Corradini, P.; Bassi, I. *Makromol. Chem.* **1960**, *37*, 156.
(14) Furukawa, J.; Saegusa, T.; Fujii, H.; Kawasaki, A.; Imai, H.; Fujii, Y. *Makromol. Chem.* **1960**, *37*, 149.
(15) (a) Furukawa, J.; Saegusa, T.; Tsuruta, H.; Fujii, H.; Tatano, T. *J. Polym. Sci.* **1959**, *36*, 546. (b) Furukawa, J.; Saegusa, T.; Tsuruta, T.; Fujii, H.; Kawasaki, A.; Tatano, T. *Makromol. Chem.* **1959**, *33*, 32.
(16) Hisatsume, I. C. *Spectrochim. Acta* **1983**, *39A*, 853.
(17) Madix, R. J.; Yamada, T.; Johnson, S. W. *Appl. Surf. Sci.* **1984**, *19*, 43.
(18) Mitchell, G. E.; Radloff, P. L.; Greenlief, C. M.; Henderson, M. A.; White, J. M. *Surf. Sci.* **1987**, *183*, 403.